

HETEROCYCLES, Vol. 93, No. 1, 2016, pp. 453 - 464. © 2016 The Japan Institute of Heterocyclic Chemistry
Received, 16th September, 2015, Accepted, 6th November, 2015, Published online, 17th November, 2015
DOI: 10.3987/COM-15-S(T)58

COMPARING THE EXTRACTION OF Am(III), Cm(III) AND Eu(III) BY CYMe₄-BTPHEN-FUNCTIONALIZED SILICA AND ZIRCONIA-COATED MAGNETIC NANOPARTICLES

James Westwood,^a Ashfaq Afsar,^a Laurence M. Harwood,^{a,*} Michael J. Hudson,^a Jan John,^b and Petr Distler^b

^aSchool of Chemistry, University of Reading, Whiteknights, Reading, Berkshire RG6 6AD, UK. E-mail: l.m.harwood@reading.ac.uk

^bDepartment of Nuclear Chemistry, Czech Technical University in Prague, Břehová 7, 11519 Prague 1, Czech Republic. E-mail: jan.john@fifi.cvut.cz

Abstract – Herein, we report the synthesis of CyMe₄-BTPhen-functionalized zirconia-coated (ZrO₂) maghemite (γ -Fe₂O₃) magnetic nanoparticles (MNPs) and their ability to extract Am(III) from Eu(III) and Am(III) from Cm(III) in a range of HNO₃ concentrations (0.001 – 4 M). Their extraction behavior is compared to our previously tested model based on silica-coated (SiO₂) MNPs. Extraction of Am(III) and Eu(III) is reported, but little or no selectivity can be seen between Am(III) and Cm(III) at concentrations of 4 M HNO₃.

Developments in the waste management of radioactive high-level liquid waste (HLLW) streams produced in the back-end of the nuclear fuel cycle will further develop public approval of nuclear power as an alternative to the combustion of depleting supplies of fossil fuels. Although only contributing to 0.1% of the spent fuel by mass, the minor actinides (Np, Am and Cm) significantly contribute to the relative radiotoxicity of nuclear waste.¹⁻³ An important step in closing the back-end of the nuclear fuel cycle may involve partitioning and transmutation (P & T) of irradiated nuclear fuel. The most successful ligands used for this process contain a number of soft donor atoms such as nitrogen and sulfur,⁴⁻⁷ because these ligands have been found to exploit the slightly more covalent nature of the metal-ligand bonding upon interaction with the minor actinide 5*f* orbitals. Liquid-liquid extraction using hydrophobic nitrogen-based ligands has proven to be the most successful method to date for partitioning of minor actinides from the remaining fission products (mainly lanthanides) in the acidic post-PUREX waste streams. In order to implement this approach two sequential partitioning processes have been proposed, which are to be

applied to the post-PUREX raffinate. The first process is to co-separate the trivalent actinides and lanthanides together by a diamide-based ligand (DIAMEX), followed by a second process involving the selective removal of the trivalent actinides (SANEX).⁸⁻¹⁰

Two promising classes of ligands that initially emerged for the selective extraction (SANEX) process were the terdentate 2,6-bis(1,2,4-triazin-3-yl)pyridine ligands (BTP's, *e.g.* CyMe₄-BTP **1**) and the quadridentate 6,6'-bis(1,2,4-triazin-3-yl)-2,2'-bipyridine ligands (BTBP's, *e.g.* CyMe₄-BTBP **2**) (Figure 1). Further modifications, primarily to improve kinetics, led to the development of bis-triazinylphenanthroline (CyMe₄-BTPhen **3**) ligands, using the 1,10-phenanthroline core to constrain the bipyridine sub-unit into the ligating orientation.¹¹⁻¹⁴ It has been previously shown that CyMe₄-BTPhen (**3**) is highly selective for Am(III) over Eu(III) in a solvent extraction protocol.¹¹

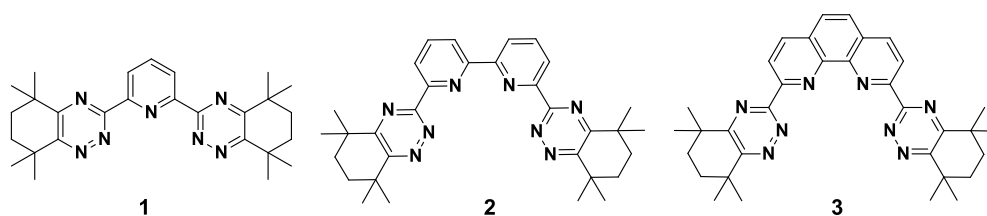


Figure 1. Structures of CyMe₄-BTP (**1**), CyMe₄-BTBP (**2**) and CyMe₄-BTPhen (**3**)

More recently, substitution at different positions of the 1,10-phenanthroline core has provided the ability to fine-tune the ligands electronically to be more selective towards actinides over lanthanides.¹⁵ The ligand efficiency for the extraction of the actinides Am(III) and Cm(III) by some electronically modulated ligands has been reported.¹⁶ Br-CyMe₄-BTPhen (**4**) and 5-(4-hydroxyphenyl)-CyMe₄-BTPhen (**5**) (Figure 2) were shown to exhibit selectivity for Am(III) over Cm(III).

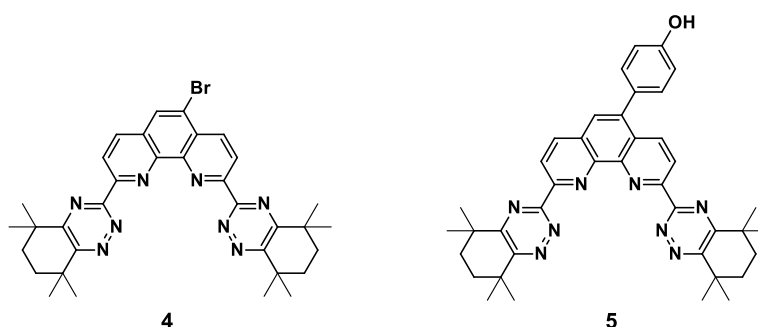


Figure 2. Structures of Br-CyMe₄-BTPhen (**4**) and 5-(4-hydroxyphenyl)-CyMe₄-BTPhen (**5**)

These molecules provide a means of amplifying the very small differences in the covalent interactions of Am(III) and Cm(III) with the ligands. Introduction of a bromine substituent at the 5-position of the

phenanthroline core, and subsequent Suzuki coupling with a 4-hydroxyphenol linker group enabled immobilisation of the CyMe₄-BTPhen ligands onto solid supports, most notably magnetic nano-particles (MNPs), where covalent attachment of C1-BTPhen ligands onto MNPs has been previously reported.¹⁷

Mono-dispersed MNPs (Fe₃O₄ or γ -Fe₂O₃) with particle sizes of less than 40 nm, offer large surface areas coupled with high surface activity. Their magnetic properties enable them to be easily separated from the supernatant solution by means of an external magnet, making them highly useful for novel separation processes.¹⁸ However, since the iron oxide core of the MNPs is prone to chemical attack under the harsh acidic conditions of the nuclear waste streams, a suitable protective coating is essential.¹⁹ An effective solution to this problem is to coat the iron oxide centre with zirconia (ZrO₂) or silica (SiO₂), both of which have been shown to provide a chemically resistant surface whilst retaining the ion-exchange properties.²⁰ Upon coating the MNPs, the free Zr-OH and Si-OH surface groups enable effective attachment of ligands through organic functional groups onto the surface of the coated MNPs. It has been previously reported²¹ that CyMe₄-BTPhen-functionalized silica-coated MNPs (Figure 3) show quantitative separation of Am(III) from Eu(III) in 0.001 – 4 M HNO₃ solutions. In addition, a small but significant selectivity for Am(III) over Cm(III) has been observed at concentrations of 4 M HNO₃.²¹ Herein, we report the synthesis of CyMe₄-BTPhen-functionalized zirconia-coated (ZrO₂) maghemite (γ -Fe₂O₃) magnetic nanoparticles (MNPs) and their ability to extract Am(III) from Eu(III) and Am(III) from Cm(III) in a range of HNO₃ concentrations (0.001 – 4 M).

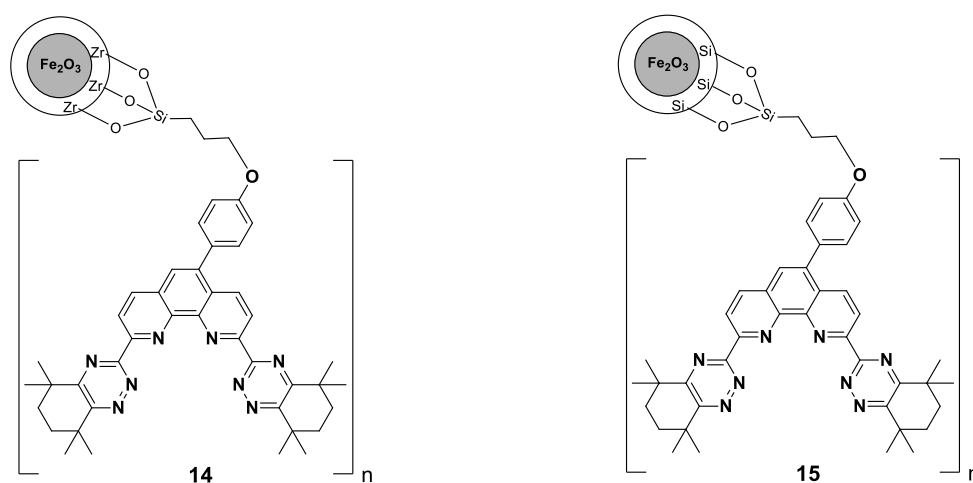


Figure 3. CyMe₄-BTPhen-functionalized ZrO₂-MNPs (**14**) and CyMe₄-BTPhen-functionalized SiO₂-MNPs (**15**)

Transmission electron microscopy (TEM) images of ZrO₂-coated MNPs revealed the thickness of the zirconia coating to be *ca.* 40-45 nm, as previously reported.¹⁷ Zirconia has a wide-ranging iso-electric

point of pH 4-11²² with the result that, in the acidic media used, the particles are protonated and have a net positive charge. The repulsion between the positively charged particles presumably ensures that there is no aggregation, increasing surface activity.²³

Immobilization of the CyMe₄-BTPPhen ligand onto ZrO₂-MNPs was followed by FT-IR where disappearance of the C-I stretch at 688 cm⁻¹ and the presence of C=C aromatic stretches at 1500-1600 cm⁻¹ were indicative of covalent attachment.¹⁷ The FT-IR spectra of both CyMe₄-BTPPhen-functionalized ZrO₂-MNPs (**14**) and CyMe₄-BTPPhen-functionalized SiO₂-MNPs (**15**) are shown in Figure 4. Both follow the same trend, but a clear difference is the more apparent broad OH absorption at 3400 cm⁻¹ for the ZrO₂-MNPs, indicative that there are residual OH groups present after covalent attachment of the ligand; indicating less efficient incorporation of the CyMe₄-BTPPhen ligand onto the MNPs surface.

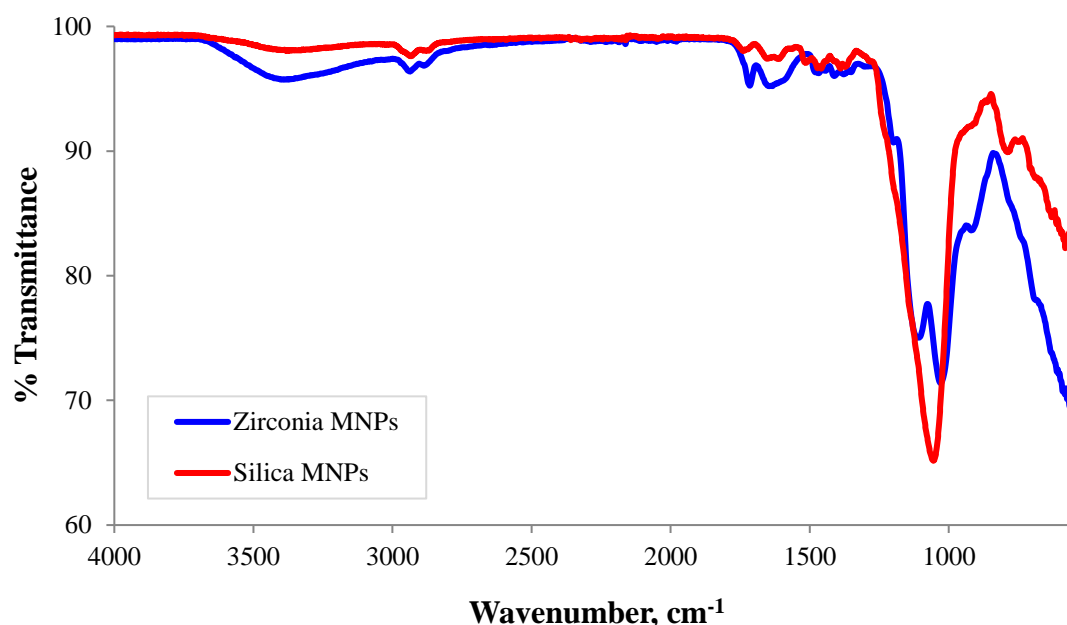


Figure 4. Comparison of the FT-IR spectra of CyMe₄-BTPPhen-functionalized ZrO₂-MNPs (**14**) and CyMe₄-BTPPhen-functionalized SiO₂-MNPs (**15**)

Elemental analysis was also used to evaluate surface incorporation of the ligand onto the MNPs. Percentage elemental composition of C, H, N and I for **14** and **15** are shown in Table 1. The results strongly indicate that there is a lower incorporation of the ligand onto the MNPs surface in the case for ZrO₂ compared with that of SiO₂. For instance, analysis of the **14** indicates 1.80% N compared to 3.43% N for **15**.

The organic content on **14** was further investigated using Thermogravimetric analysis (TGA) under nitrogen (Figure 5). A similar trend compared with previously studied **15** is reported, where below 150 °C

the mass loss was quite small, owing to removal of absorbed water and a near linear mass loss was observed between ca. 250-700 °C, probably due to the decomposition of the organic content.

Table 1. Results of elemental analysis for CyMe₄-BTPPhen-functionalized ZrO₂-MNPs (**14**) and CyMe₄-BTPPhen-functionalized SiO₂-coated MNPs (**15**)

	CyMe ₄ -BTPPhen-functionalized ZrO ₂ -MNPs (14)		CyMe ₄ -BTPPhen-functionalized SiO ₂ -MNPs (15)	
	Experimental	Theoretical	Experimental	Theoretical
C (%)	17.16	22.79	23.20	22.79
H (%)	3.37	2.14	3.48	2.14
N (%)	1.80	4.94	3.43	4.94
I (%)	7.69	0	8.28	0

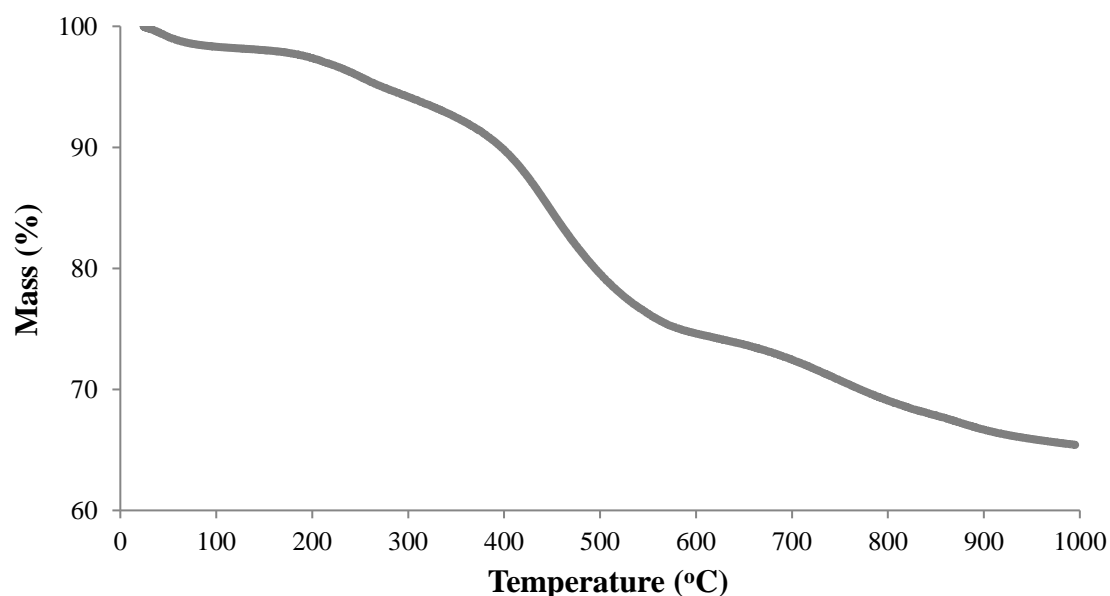


Figure 5. TGA curve for CyMe₄-BTPPhen-functionalized ZrO₂-MNPs (**14**)

The extraction results obtained for **14** showed good distribution ratios for both Am(III) ($D_{Am} = 142 \pm 4$) and Eu(III) ($D_{Eu} = 9.7 \pm 4.2$) at 0.001 M HNO₃ with a separation factor of $SF_{Am/Eu} = 14.7 \pm 1.4$ (Table 2). However, these values are much lower than those obtained for the same ligand covalently bound in the same manner to SiO₂-MNPs ($D_{Am} = 1168.8 \pm 79.1$ and $D_{Eu} = 701.4 \pm 32.4$).²¹ Increasing HNO₃ concentration to 0.1 M showed a dramatic decrease in both Am(III) extraction ($D_{Am} = 5.6 \pm 1$), and Eu(III) extraction ($D_{Eu} = 0.8 \pm 0.1$) giving a separation factor of $SF_{Am/Eu} = 7.4 \pm 7.5$ at 0.1 M HNO₃. In the case for the CyMe₄-BTPPhen-functionalized SiO₂-MNPs however, an increase in the extraction of Am(III) at 0.1 M HNO₃ was reported $D_{Am} = 1857 \pm 153.5$ whilst Eu(III) extraction decreased to $D_{Eu} =$

101.1 ± 2.3 giving a $SF_{Am/Eu} = 18.4 \pm 1.6$.²¹ A linear decrease in both Am(III) and Eu(III) extraction was observed for **14** upon increasing HNO_3 concentration to both 1 M and 4 M (Figure 6). Although D_{Am} remained greater than D_{Eu} in both cases the selectivity was all but lost at 4 M HNO_3 solution with $D_{Am} = 0.8 \pm 0.9$ and $D_{Eu} = 0.4 \pm 0.9$ resulting in $SF_{Am/Eu} = 1.8 \pm 0.4$. This is significantly lower than the results obtained for **15** at 4 M HNO_3 where a $SF_{Am/Eu} = \approx 1700 \pm 300$ was obtained.²¹

Table 2. Extraction of Am(III) and Eu(III) by $CyMe_4-BTPhen$ ZrO_2 -MNPs (**14**) as a function of nitric acid concentration (* gamma measurement)

[HNO_3]	D_{Am}^*	D_{Eu}^*	$SF_{Am/Eu}$
0.001	142 ± 4.0	9.7 ± 4.2	14.7 ± 1.4
0.1	5.6 ± 1.0	0.8 ± 1.0	7.4 ± 7.5
1	1.4 ± 0.9	0.7 ± 0.9	2.0 ± 1.7
4	0.8 ± 0.9	0.4 ± 0.9	1.8 ± 0.4

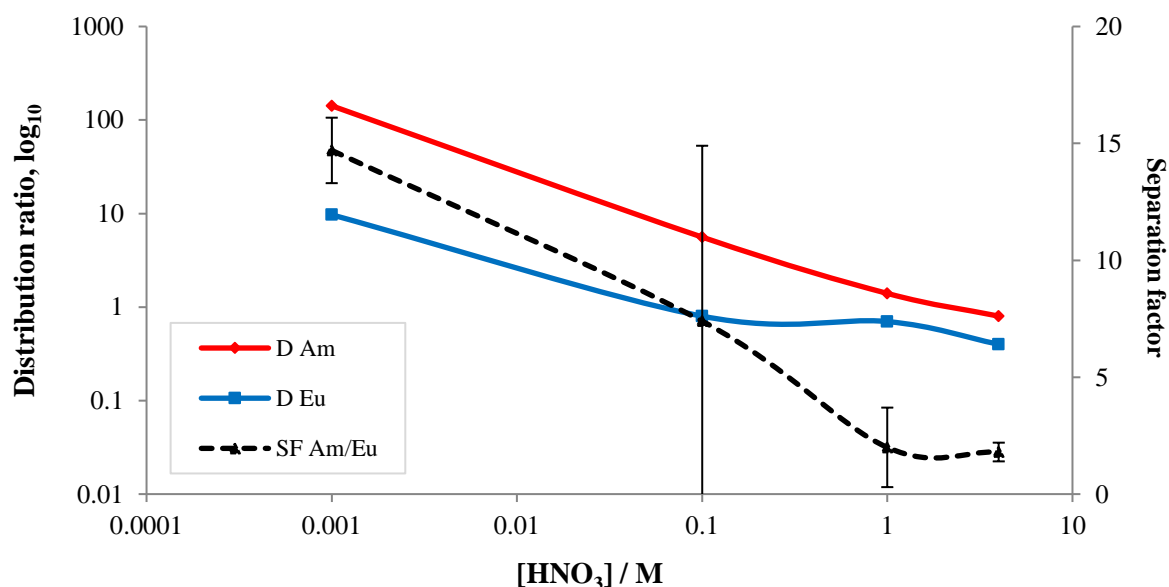


Figure 6. Extraction of Am(III) and Eu(III) by $CyMe_4-BTPhen$ ZrO_2 -MNPs (**14**) as a function of nitric acid concentration

Distribution ratios for the actinides Am(III) and Cm(III) and the resulting separation factors at 0.001 – 4 M HNO_3 by **14** were also examined (Table 3). The D values for both Am(III) and Cm(III) decreased upon increasing HNO_3 concentration, with little or no selectivity observed at 4 M HNO_3 with a $SF_{Am/Cm} = 0.7 \pm 0.1$. These values follow the same trend as for **15**, but show much lower D and SF values across all concentrations were attained. **15** produced a $SF_{Am/Cm} = 2.2 \pm 0.4$ at 4 M HNO_3 , a significant separation;²¹ whereas **14** across all concentrations showed $SF_{Am/Cm}$ that barely rose above 1 (Figure 7).

Table 3. Extraction of Am(III) and Cm(III) by CyMe₄-BTPPhen ZrO₂-MNPs (**14**) as a function of nitric acid concentration (** alpha measurement)

[HNO ₃]	D_{Am}^{**}	D_{Cm}^{**}	$SF_{Am/Cm}$
0.001	185 ± 13	145 ± 10	1.3 ± 0.1
0.1	12.7 ± 2.6	10.7 ± 2.6	1.2 ± 0.4
1	4.3 ± 2.3	5.7 ± 2.4	0.8 ± 0.5
4	3.0 ± 2.3	4.4 ± 2.3	0.7 ± 0.1

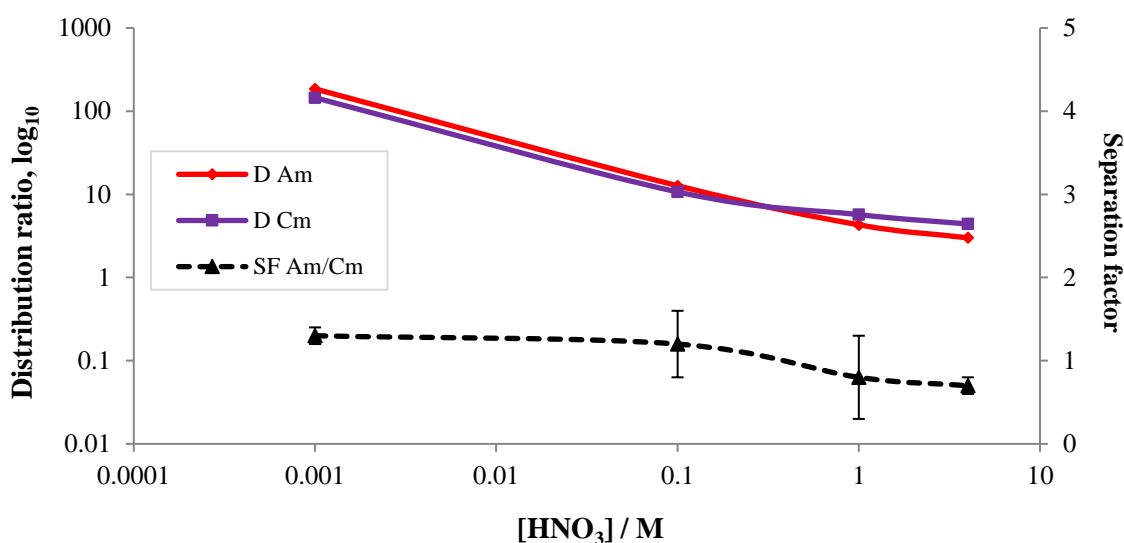


Figure 7. Extraction of Am(III) and Cm(III) by CyMe₄-BTPPhen ZrO₂-MNPs (**14**) as a function of nitric acid concentration

In summary, a convenient route for immobilisation of CyMe₄-BTPPhen ligands via a phenyl ether linkage onto the surface of zirconia-coated maghemite (γ -Fe₂O₃) magnetic nanoparticles is reported. These MNPs successfully co-extracted both Am(III) and Eu(III) from solutions up to 4 M HNO₃, with low selectivity ($SF_{Am/Eu} = 1.8$) compared to that previously for reported SiO₂-coated MNPs ($SF_{Am/Eu} = > 1300$). Extraction of both actinides Am(III) and Cm(III) is also noted, again without any selectivity; whereas previously reported SiO₂-coated MNPs exhibited a significant selectivity for Am(III) over Cm(III) ($SF_{Am/Eu} = 2.2$ at 4 M HNO₃). Based on FT-IR and elemental analysis data, the surface of the ZrO₂-MNPs appears to be less functionalized with CyMe₄-BTPPhen ligands than the SiO₂-MNPs counterpart. Both ZrO₂- and SiO₂ provide an effective coating to the iron oxide core to enable chemical resistance to the harsh conditions in extraction processes, but since the SiO₂-MNPs can incur high ligand loading, we conclude that SiO₂-MNPs will be favoured over ZrO₂-MNPs for future investigations to provide an effective extraction from SANEX-type processes.

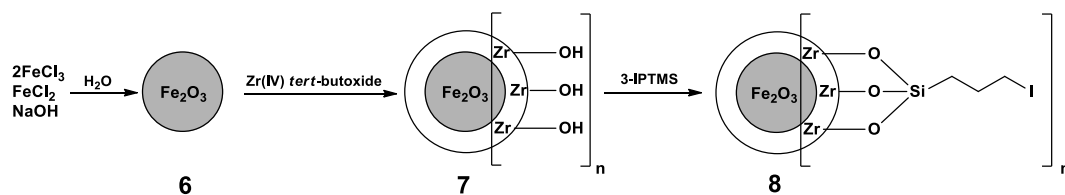
EXPERIMENTAL

Materials. Iron(III) chloride, iron(II) chloride tetrahydrate, sodium hydroxide pellets, ammonium hydroxide (35%), zirconium (IV) *tert*-butoxide, 3-iodopropyltrimethoxysilane (3-IPTMS), ethanol and dimethylformamide (DMF) were purchased from Sigma-Aldrich. All chemicals were of analytical grade and used as received without further purification. Degassed deionized water was used throughout the experiment.

Characterization. The size and morphology of the MNPs at various stages of functionalization were observed by Philips/FEI CM20 transmission electron microscopy and samples were obtained by placing a drop of colloid solution onto a copper grid and allowing evaporation in air at room temperature. Thermo-gravimetric (TGA) analyses were performed using a TGA-Q50 thermo-gravimetric analyzer. IR spectra were recorded as Nujol® mulls (N) on a Perkin Elmer RX1 FT-IR instrument.

Extraction studies. The aqueous solutions for the solvent extraction experiments were prepared by spiking nitric acid solutions (0.745 mL) (0.001 – 4 M) with stock solutions of 5 μL of ^{241}Am (≈ 400 Bq/ μL), 3 μL of ^{152}Eu (≈ 1.000 Bq/ μL), and 7 μL of ^{244}Cm (≈ 300 Bq/ μL) and then adding 600 μL of spiked aqueous solution to 18 mg of **14**. 150 μL of each labelled solution was taken as a standard (to allow mass balance calculations) for γ -measurements and 10 μL was taken as a standard for α -measurements. The suspension was sonicated for 10 min and shaken on a Heidolph Reax shaker at 1800 rpm for 90 min. After centrifuging for 10 min, aliquots of the aqueous solutions (supernatant) were separated and taken for measurements. Activity measurements of ^{241}Am , ^{152}Eu and ^{244}Cm were performed with a γ -ray spectrometer EG&G Ortec (USA) with a PGT (USA) HPGe detector and α -ray spectrometer Octete plus Ortec (Germany) with ion-implanted-silicon ultra α -detector (USA). The distribution ratios, D , were calculated as the ratio between the radioactivity (α - and γ -emissions) of each isotope in the standard solution and the supernatants after removal of the **14** complexes. The separation factor is $SF_{\text{Am/Eu}} = D_{\text{Am}} / D_{\text{Eu}}$ or $SF_{\text{Am/Cm}} = D_{\text{Am}} / D_{\text{Cm}}$. Extractions were studied at nitric acid concentrations of 0.001 M, 0.1 M, 1 M and 4 M. All extraction experiments were carried out in duplicate and error bars in the figures represent standard deviations.

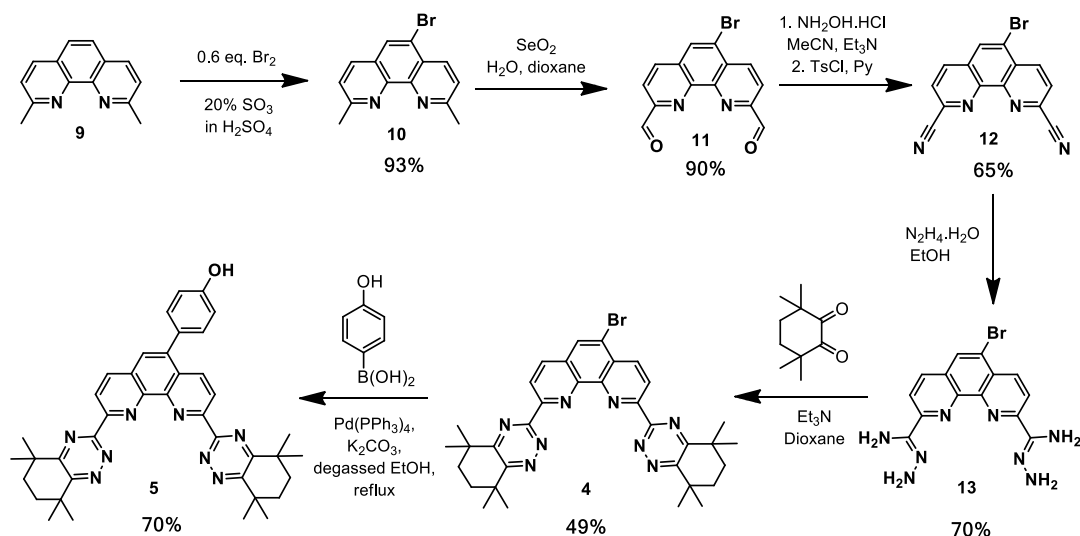
Synthesis of Iodoalkyl-functionalized ZrO₂-Coated Fe₂O₃ MNPs (8). Following the literature procedure,²⁴⁻²⁷ complete precipitation of Fe₂O₃ was achieved under alkaline conditions, while maintaining a molar ratio of Fe²⁺:Fe³⁺ = 1:2 under nitrogen (Scheme 1).



Scheme 1. Synthesis of iodo-functionalized zirconia-coated γ -Fe₂O₃ MNPs (**8**)

To obtain 0.70 g of Fe₂O₃ MNPs **6**, FeCl₂·4H₂O (0.80 g, 4 mmol) and FeCl₃ (1.30 g, 8 mmol) dissolved in degassed deionized water 40 mL were added dropwise into 2M NaOH solution (200 mL) with vigorous stirring. After 1 h, the resulting Fe₂O₃ MNPs (**6**) were separated by putting the vessel on a neodymium magnet and decanting the supernatant. The MNPs (**6**) were washed with degassed deionized water (2 × 100 mL) and 0.01M HCl (17%, 100 mL) to remove unreacted iron salts. Fe₂O₃ MNPs (**6**) were then coated with ZrO₂ using a sol-gel method.²⁴⁻²⁷ Typically, Fe₂O₃ MNPs (**6**) (0.70 g) were dispersed in a mixed solution of degassed ethanol (300 mL) and degassed deionized water (75 mL) by sonication for 10 min. Ammonium hydroxide (35%, 36 mL) and zirconium (IV) *tert*-butoxide (5.1 mL) were consecutively added to reaction mixture and the reaction was allowed to proceed at room temperature for 2 h under continuous sonication. (3-Iodopropyl)trimethoxysilane (6.3 mL) was then added and the reaction was allowed to proceed for further 3 h. The resultant functionalized particles (**8**) were obtained by magnetic separation and thoroughly washed with degassed ethanol (4×250 mL). Finally the resultant yellow powder (9.30 g) was dried at 120 °C.

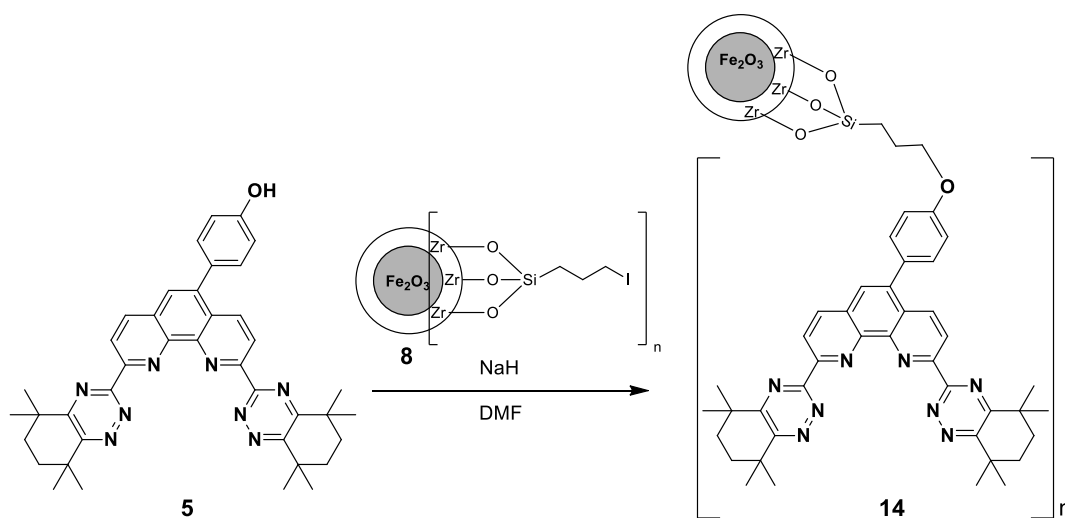
Synthesis of 5(4-hydroxyphenyl)-CyMe₄-BTPPhen (5**).** 5(4-Hydroxyphenyl)-CyMe₄-BTPPhen (**5**) was synthesized using our previously reported procedure, summarized in Scheme 2.^{15,16,21,28}



Scheme 2. Synthesis of 5(4-hydroxyphenyl)-CyMe₄-BTPPhen (**5**)

Commercially available 2,9-dimethyl-1,10-phenanthroline (neocuproine) (**9**) was firstly regioselectively brominated²⁹ using 0.6 equivalents of bromine in fuming sulfuric acid to give the 5-bromo species (**10**). Oxidation using selenium dioxide in 1,4-dioxane gave the dialdehyde (**11**) followed by a one-pot transformation into the dinitrile (**12**). Stirring the dinitrile in hydrazine hydrate and EtOH yields bis-aminohydrazide (**13**) before condensation with CyMe₄ diketone furnishing the Br-CyMe₄-BTPhen ligand (**4**). Replacement of the bromine with a 4-hydroxyphenyl linking group was successfully achieved via Suzuki coupling³⁰ with 4-hydroxyphenylboronic acid.

Synthesis of CyMe₄-BTPhen functionalized ZrO₂-Coated MNPs (14**).** Immobilisation of CyMe₄-BTPhen on MNPs was carried out in DMF in the presence of sodium hydride as shown in Scheme 3. Sodium hydride (60% dispersion in mineral oil, 0.03 g, 0.9 mmol, 1.3 eq) was added to a solution of 5(4-hydroxyphenyl)-CyMe₄-BTPhen **5** (0.46 g, 0.7 mmol) in DMF (100 mL) at 120 °C and stirred for 30 min. Iodoalkyl-functionalized ZrO₂-coated MNPs (**8**) (0.72 g) were slowly added and the reaction mixture was stirred at 120 °C overnight. CyMe₄-BTPhen-functionalized MNPs (**14**) were separated by an external magnet and were thoroughly washed with degassed EtOH (3×100 mL). Finally, the product (0.24 g) was allowed to dry at 120 °C.



Scheme 3. Immobilisation of 5(4-hydroxyphenyl)-CyMe₄-BTPhen (**5**) on MNPs (**8**)

ACKNOWLEDGEMENTS

Use of the Chemical Analysis Facility (CAF) at the University of Reading is also gratefully acknowledged. All data supporting this study are reported in this paper. Any enquiries about the data should be addressed to the corresponding author.

REFERENCES

1. F. W. Lewis, M. J. Hudson, and L. M. Harwood, *Synlett*, 2011, **2609**.
2. Z. Kolarik, *Chem. Rev.*, 2008, **108**, 4208.
3. P. J. Panak and A. Geist, *Chem. Rev.*, 2013, **113**, 1199.
4. C. Madic, B. Boullis, P. Baron, R. Testard, M. J. Hudson, J. O. Lijenzin, B. Christiansen, M. Ferrando, A. Facchini, A. Geist, G. Modolo, A. G. Espartero, and J. De Mendoza, *J. Alloys Compd.*, 2007, **444**, 23.
5. M. P. Jensen and A. H. Bond, *J. Am. Chem. Soc.*, 2002, **124**, 9870.
6. T. Guoxin, Z. Yongjun, X. Jingming, Z. Ping, H. Tiandou, X. Yaning, and Z. Jing, *Inorg. Chem.*, 2003, **42**, 735.
7. H. H. Dam, D. N. Reinhoudt, and W. Verboom, *Chem. Soc. Rev.*, 2007, **36**, 367.
8. A. Fermvik, C. Ekberg, S. Englund, M. R. S. J. Foreman, G. Modolo, T. Retegan, and G. Skarnemark, *Radiochim. Acta*, 2009, **97**, 319.
9. A. E. V. Gorden, M. A. DeVore, and B. A. Maynard, *Inorg. Chem.*, 2012, **52**, 3445.
10. M. J. Hudson, F. W. Lewis, and L. M. Harwood, *Strategies and Tactics in Organic Synthesis*, Academic Press, 2013, **9**, pp. 177-202.
11. F. W. Lewis, L. M. Harwood, M. J. Hudson, M. G. Drew, J. F. Desreux, G. Vidick, N. Bouslimani, G. Modolo, A. Wilden, M. Sypula, T. H. Vu, and J. P. Simonin, *J. Am. Chem. Soc.*, 2011, **133**, 13093.
12. Z. Kolarik, U. Müllich, and F. Gassner, *Solvent Extr. Ion Exch.*, 1999, **17**, 23.
13. F. W. Lewis, L. M. Harwood, M. J. Hudson, M. G. B. Drew, V. Hubscher-Bruder, V. Videva, F. Arnaud-Neu, K. Stamberg, and S. Vyas, *Inorg. Chem.*, 2013, **52**, 4993.
14. M. J. Hudson, L. M. Harwood, D. M. Laventine, and F. W. Lewis, *Inorg. Chem.*, 2012, **52**, 3414.
15. A. Afsar, D. M. Laventine, L. M. Harwood, M. J. Hudson, and A. Geist, *Chem. Commun.*, 2013, **49**, 8534.
16. A. Afsar, L. M. Harwood, M. J. Hudson, J. Westwood, and A. Geist, *Chem. Commun.*, 2015, **51**, 5860.
17. L. M. Harwood, A. Afsar, D. L. Laventine, M. J. Hudson, and A. Geist, *Heterocycles*, 2014, **88**, 613.
18. A.-F. Ngomsik, A. Bee, D. Talbot, and G. Cote, *Sep. Purif. Technol.*, 2012, **86**, 1.
19. Z. Y. Ma, Y. P. Guan, and H. Z. Liu, *J. Magn. Magn. Mater.*, 2006, **301**, 469.
20. Y. Q. Hu, S. X. Zhou, and L. M. Wu, *Polymer*, 2009, **50**, 3609.
21. A. Afsar, L. M. Harwood, M. J. Hudson, P. Distler, and J. John, *Chem. Commun.*, 2014, **50**, 15082.

22. M. Schultz, S. Grimm, and W. Burckhardt, [*Solid State Ionics*, 1993, **63–65**, 18.](#)
23. M. Kaur, H. Zhang, L. Martin, T. Todd, and Y. Qiang, [*Environ. Sci. Technol.*, 2013, **47**, 11942.](#)
24. A. L. Morel, S. I. Nikitenko, K. Gionnet, A. Wattiaux, J. Lai-Kee-Him, C. Labrugere, B. Chevalier, G. Deleris, C. Petibois, A. Brisson, and M. Simonoff, [*ACS Nano*, 2008, **2**, 847.](#)
25. J. H. Jang and H. B. Lim, [*Microchem. J.*, 2010, **94**, 148.](#)
26. M. Nazrul Islam, L. Van Phong, J.-R. Jeong, and C. Kim, [*Thin Solid Films*, 2011, **519**, 8277.](#)
27. F. W. Zhang, Z. Z. Zhu, Z. P. Dong, Z. K. Cui, H. B. Wang, W. Q. Hu, P. Zhao, P. Wang, S. Y. Wei, R. Li, and J. T. Ma, [*Microchem. J.*, 2011, **98**, 328.](#)
28. D. M. Laventine, A. Afsar, M. J. Hudson, and L. M. Harwood, [*Heterocycles*, 2012, **86**, 1419.](#)
29. J. Mlochowski, *J. Rocz. Chem.*, 1974, **48**, 2145.
30. J. P. W. Eggert, U. Luning, and C. Nather, [*Eur. J. Org. Chem.*, 2005, 1107.](#)